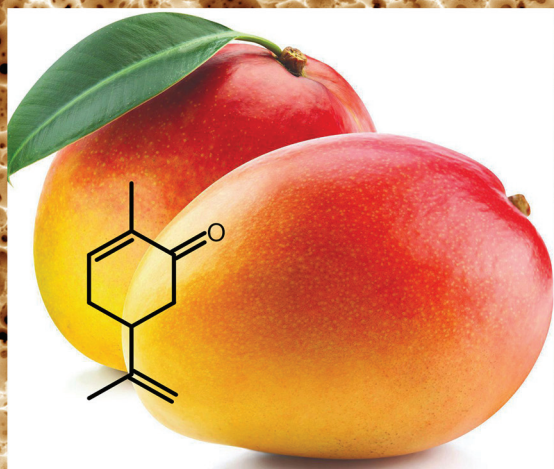


Polymer Chemistry

Volume 14
Number 12
28 March 2023
Pages 1287-1406

rsc.li/polymers



ISSN 1759-9962

PAPER

Peter Krajnc *et al.*

Terpenes as natural building blocks for the synthesis of hierarchically porous polymers: bio-based polyHIPEs with high surface areas



Cite this: *Polym. Chem.*, 2023, **14**, 1330

Terpenes as natural building blocks for the synthesis of hierarchically porous polymers: bio-based polyHIPEs with high surface areas†

Stanko Kramer,  Nika Skušek and Peter Krajnc  *

PolyHIPEs are hierarchically porous polymers which are generally synthesised from synthetic constituents produced from fossil fuels. The need to produce sustainable materials makes terpenes great candidates for the preparation of polyHIPEs as they possess polymerisable functionalities, while being abundant in various plants and flowers. In this study limonene, carvone and myrcene are used to produce bio-based polyHIPEs by utilising multifunctional acrylates (trimethylol propane triacrylate (TMPTA) and pentaerythritol tetraacrylate (PETA)) as the comonomers in the polymerisation process. By using the two monomer units it was possible to synthesise poly(limonene-co-TMPTA), poly(limonene-co-PETA), poly(carvone-co-TMPTA), poly(carvone-co-PETA), poly(myrcene-co-TMPTA) and poly(myrcene-co-PETA) HIPEs. The terpene and acrylate ratios are varied to study the incorporation of the terpenes into the polyHIPE and the effects on the morphological properties. While the synthesis of terpene-based polyHIPEs was successful, the degree of limonene and carvone incorporation reduces when the content thereof in the HIPE mixture is increased. The synthesised polyHIPEs had a pore diameter ranging from 5.51 to 11.63 μm , while the specific surface area ranged from 2.7 $\text{m}^2 \text{g}^{-1}$ and up to approximately 300 $\text{m}^2 \text{g}^{-1}$. This study is the first study that demonstrates the possibility of preparing polyHIPEs from limonene and carvone. Additionally, it shows that it is possible to synthesise porous polymers from sustainable constituents.

Received 15th December 2022,
Accepted 31st January 2023

DOI: 10.1039/d2py01566h

rsc.li/polymers

Introduction

In the year 2021 only about 2 million tonnes of the more than 375 million tonnes of the produced plastics came from renewable resources.^{1,2} Additionally, the ever-increasing price of fossil fuels also results in an increase of the overall living costs, while heavily polluting the environment and endangering human life.³ Therefore, it is necessary to use more sustainable raw materials to produce polymers, for example, plant-based resources.⁴

Besides the general use of various polymers in different industries they can also be used in more specialised/advanced cases. For example, they can be used for wastewater treatment,⁵ catalysis,⁶ as biosensors and sensors,⁷ as stimuli-responsive materials⁸ and in various biomedical applications,⁹ to name a few. Among these polymers, there is a special class of polymers known as porous polymers. Their inherent porosity gives them certain advantages when compared to non-porous polymers, especially their permeability and their three-

dimensional structure.¹⁰ Among porous polymers there is a sub-class of porous polymers which are produced through emulsion templating known as polyHIPEs (polymerised high internal phase emulsions). PolyHIPEs are produced by polymerising HIPEs (high internal phase emulsions), which are emulsions with an internal phase volume of at least 74.05 vol%. The most common HIPEs are either water-in-oil (w/o) or oil-in-water (o/w) emulsions.¹¹ PolyHIPEs have the same inherent disadvantage as other polymers, namely their unsustainability. Generally, polyHIPEs are produced from styrene, divinylbenzene, different acrylates, urethanes, thiols, dicyclopentadiene and norbornene, to name a few.¹² However, polyHIPEs have also been produced from polysaccharides. For example, gelatine, dextran, pullulan, alginate, cellulose and chitosan.^{13–16} Generally, these polyHIPEs have been used for biomedical applications due to their inherent biocompatibility and biodegradability.¹⁷ Besides polysaccharides other bio-based constituents have also been used to prepare porous polymers. Yang *et al.*¹⁸ used poly(L-lactic acid) to prepare biocompatible scaffolds for 3D printing and cell growth, while Foulet *et al.*¹⁹ used Kraft lignin to prepare polyHIPEs. Another group of bio-based constituents are terpenes. Terpenes consist of cycloaliphatic and aromatic structures which are also common in petroleum-based chemicals. However, unlike petroleum-

PolyOrgLab, Faculty of Chemistry and Chemical Engineering, University of Maribor, Smetanova ulica 17, 2000 Maribor, Slovenia. E-mail: peter.krajnc@um.si

† Electronic supplementary information (ESI) available. See DOI: <https://doi.org/10.1039/d2py01566h>



based chemicals they are abundant in nature and sustainable.²⁰ Among terpenes pinene, limonene and myrcene have been the most widely studied monomers for the production of polymers, whereas carvone is the most studied terpenoid. However, generally the polymerisation of these monomers leads to polymers with low molecular weights, therefore, comonomers are often used to produce polymers with higher molecular weights.²¹

Currently the only terpene utilised for the synthesis of terpene-based polyHIPEs is myrcene. Mert's group polymerised myrcene with various comonomers, namely ethylene glycol dimethacrylate (EGDMA), 1,3-butanedioldiacrylate (BDDA), divinylbenzene (DVB) and 4-vinylbenzyl chloride (VBC) to produce various polyHIPEs.^{22,23} Additionally, the polyHIPEs based on myrcene were hypercrosslinked to increase their specific surface area from 2.25 m² g⁻¹ to 60.18 m² g⁻¹,²³ modified with nanoclay to improve their mechanical properties and interconnectivity²⁴ and used for the adsorption of different organic solvents.²⁵

In this study limonene, carvone and myrcene will be used to synthesise bio-based polyHIPEs by using either trimethylolpropane triacrylate (TMPTA) or pentaerythritol tetraacrylate (PETA) as the crosslinkers. The ratio between the natural monomers and the acrylates will be varied to evaluate the inclusion of the terpenes into the polymer, while also studying the effect of the crosslinker on the properties of the obtained terpene-based polyHIPEs. This study will be the first one to use limonene and carvone as building blocks for the synthesis of polyHIPEs.

Experimental section

Materials

D,L-Limonen (Lim, Sigma-Aldrich); β -myrcene (Myr, Myrcene, Sigma-Aldrich), carvone (Carv, Sigma Aldrich); pentaerythritol tetraacrylate (PETA, Sigma-Aldrich); trimethylolpropane triacrylate (TMPTA, Sigma-Aldrich); toluene (Carlo Erba); α,α' -azoisobutyronitrile (AIBN, Sigma-Aldrich, 98%); Hypermer B246 (HB246, Croda); calcium chloride hexahydrate (Sigma Aldrich) and 2-propanol (Sigma-Aldrich) were used without further purifications.

PolyHIPE preparation

Hierarchically porous polymers (polyHIPEs) were prepared by polymerising water-in-oil high internal phase emulsions (HIPEs). The organic phase was comprised of limonene, myrcene or carvone and either TMPTA or PETA in different ratios according to Table 1. Additionally, α,α' -azoisobutyronitrile (AIBN) (2 wt%, based on the monomer weight), toluene (50 wt%, based on the monomer weight) and Hypermer B246 (4 wt%, based on the monomer weight) were also added to the organic phase. The aqueous phase was prepared by dissolving calcium chloride hexahydrate (CaCl₂·6H₂O) in degassed deionized water and added to the oil/organic phase dropwise while stirring at 400 rpm with an overhead stirrer. To obtain a

Table 1 Composition of the prepared polyHIPEs

Sample	Terpene	Acrylate	$n(\text{terpene})$ [mmol]	$n(\text{acrylate})$ [mmol]
LT1_3	Lim	TMPTA	2.5	7.5
LT1_1	Lim	TMPTA	6	6
LT3_1	Lim	TMPTA	9.9	3.3
LP1_3	Lim	PETA	2.5	7.5
LP1_1	Lim	PETA	6	6
LP3_1	Lim	PETA	10.5	3.5
CT1_3	Carv	TMPTA	2.5	7.5
CT1_1	Carv	TMPTA	6	6
CT3_1	Carv	TMPTA	9.9	3.3
CP1_3	Carv	PETA	2.5	7.5
CP1_1	Carv	PETA	6	6
CP3_1	Carv	PETA	10.5	3.5
MT1_3	Myr	TMPTA	2.5	7.5
MT1_1	Myr	TMPTA	6	6
MT3_1	Myr	TMPTA	9.9	3.3
MP1_3	Myr	PETA	2.5	7.5
MP1_1	Myr	PETA	6	6
MP3_1	Myr	PETA	10.5	3.5
T	—	TMPTA	0	9
P	—	PETA	0	8

uniform emulsion, stirring was continued for another 30 minutes after the addition of the aqueous phase. The prepared HIPE was polymerised for 24 h in an electric oven at 60 °C. A simplified scheme of the whole process is shown in Fig. 1. The exact weights of the prepared samples are shown in the ESI (Table S1†). The synthesised polyHIPEs were purified with 2-propanol for 24 hours by using a Soxhlet apparatus and then air dried for 48 hours and afterwards under vacuum at 30 °C. The samples are labelled the following way: XY_a_b, where X is the terpene used (limonene – L; carvone – C; myrcene – M), Y is the acrylate used (TMPTA – T; PETA – P), *a* represents the ratio of the terpene and *b* the ratio of acrylate (1 : 3; 1 : 1; 3 : 1). Therefore, LT1_3 would represent a poly(limonene-co-TMPTA) polyHIPE with a limonene to terpene ratio of 1 : 3.

Characterisation

The morphology was analysed with a Philips XL series scanning electron microscope (SEMTEch Solutions, MA, USA). Subsequently, the diameter of the cavities and the windows was measured by using the image processing programme ImageJ. At least 100 pores were measured for each sample and the correction factor of $2/\sqrt{3}$ was applied, as the measured diameters are otherwise underestimates of the actual values due to the random sectioning.²⁶ The porosity was determined by measuring the overall density using the Micromeritics GeoPyc 1365 envelope & density analyser (Micromeritics, Unterschleißheim, Germany) and skeletal density using the AccuPyc II 1345 gas displacement pycnometry system (Micromeritics, Unterschleißheim, Germany). The specific surface area (BET) was measured by using the Micromeritics TriStar II 3020 surface area and porosity system (Micromeritics, Unterschleißheim, Germany). Prior the measurement the samples were degassed at 40 °C for 24 hours



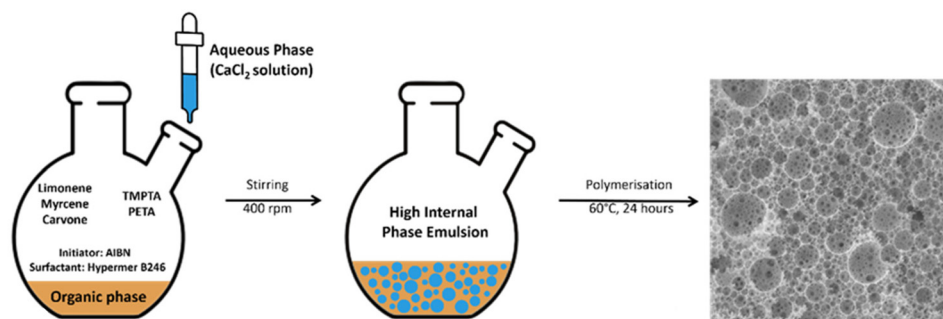


Fig. 1 Simplified representation of the preparation of polyHIPEs.

by using the FlowPrep 060 gas adsorption sample preparation device (Micromeritics, Unterschleißheim, Germany). The FTIR spectra were recorded on the PerkinElmer spectrum 3 tri-range MIR/NIR/FIR spectrometer (PerkinElmer, MA, USA) accessorised with the Pike GladiATR – ATR accessory (Pike Technologies, WI, USA) at a scan range between 4000 and 450 cm^{-1} . A total of 16 scans were performed at all measurements with a resolution of 4 cm^{-1} . The thermogravimetric analysis (TGA) was performed in nitrogen (20 ml min^{-1}) from 25 $^{\circ}\text{C}$ to 750 $^{\circ}\text{C}$ (10 K min^{-1}) using the thermal analysis system TGA 2 (Mettler Toledo, OH, USA). The elemental analysis was performed by using the PerkinElmer 2400 Series II CHNS/O elemental analyser (PerkinElmer, MA, USA). The yield of the polymerisations was determined gravimetrically, while the incorporation of the terpenes into the polymer was calculated from the elemental composition obtained from the elemental analyser by using eqn (1):

$$n(\text{terpene}) = \frac{N(\text{C, acrylate}) \times M(\text{C}) - M(\text{acrylate}) \times \%(\text{C})}{M(\text{terpene}) \times \%(\text{C}) - N(\text{C, terpene}) \times M(\text{C}) \times n(\text{acrylate})}, \quad (1)$$

where $\%(\text{C})$ is the wt% of carbon in the sample obtained from the elemental analyser. The number of moles for the acrylate in the equation were constant (1 mol) to enable the calculation of the number of moles for the terpene.

Results and discussion

Polymerisation

The terpenes used in this study are shown in Fig. 2. As it is difficult to prepare homopolymers from terpenes, acrylate comonomers were used to facilitate the preparation of terpene-based polyHIPEs.²¹ TMPTA and PETA were used as the comonomers. The ratio of the acrylates was varied from 100 mol% acrylate to 25 mol% acrylate. The acrylate-only polyHIPEs were prepared as a comparison to evaluate the influence of the terpene inclusion on the morphological properties in the prepared polyHIPEs. To produce porous copolymers from the terpenes and acrylates AIBN was utilised to initiate the free radical polymerisation thereof. The yields of the polymeris-

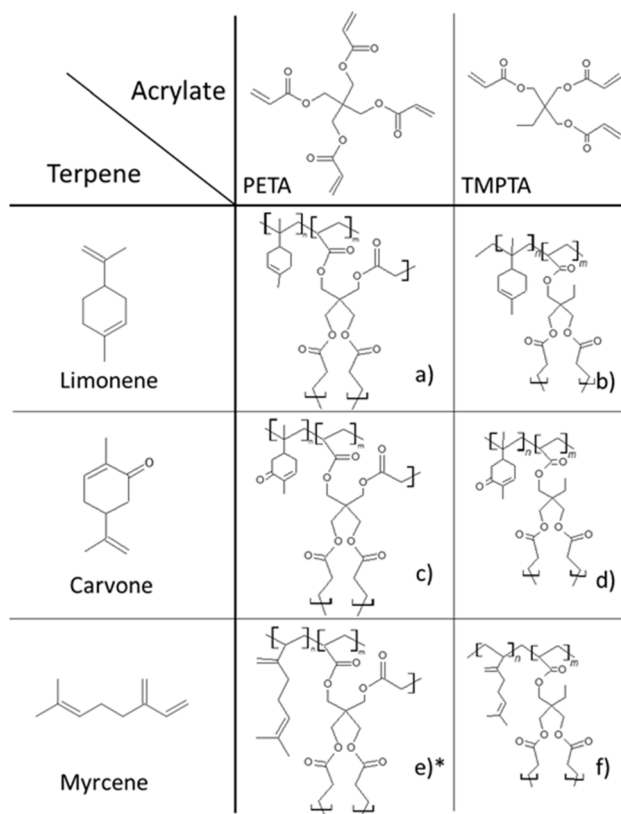


Fig. 2 Synthesised terpene-based polyHIPEs. (a) Poly(limonene-co-PETA); (b) poly(limonene-co-TMPTA); (c) poly(carvone-co-PETA); (d) poly(carvone-co-TMPTA); (e) poly(myrcene-co-PETA); (f) poly(myrcene-co-TMPTA). * The scheme representing poly(myrcene-co-TMPTA).

ations decreased with increasing terpene ratio (Table 2). For the poly(limonene-co-TMPTA) polyHIPEs the yields decreased from 87%, to 74% and to 49% (LT1_3, LT1_1 and LT3_1, respectively), while for the poly(limonene-co-PETA) polyHIPEs they decreased from 86%, to 50% and to 41% (LP1_3, LP1_1 and LP3_1, respectively). The decrease of the conversion with increased limonene content was also observed by Sharma *et al.*,²⁷ while Ren *et al.*²⁸ obtained nearly undetectable amounts of oligomers when conducting the homopolymerisation of limonene by using BPO as the initiator. This indicates



Table 2 Yields, theoretical and experimental terpene inclusion values of the synthesised polymers

Sample	Yield [%]	<i>n</i> (terpene) theoretical [mol%]	<i>n</i> (terpene) measured [mol%]	<i>C</i> ^a [%]
LT1_3	87	25.1	15.0	62.85
LT1_1	74	49.9	20.7	63.74
LT3_1	49	74.2	32.3	65.72
LP1_3	85	25.1	26.0	61.57
LP1_1	50	50.2	27.6	61.84
LP3_1	41	74.8	2.8	58.29
CT1_3	89	24.9	24.1	64.29
CT1_1	74	50.0	28.8	65.10
CT3_1	46	74.9	24.4	64.33
CP1_3	95	25.5	16.9	59.71
CP1_1	76	50.4	25.0	60.69
CP3_1	54	74.8	24.1	60.58
MT1_3	92	25.1	26.4	64.67
MT1_1	89	49.9	48.0	68.96
MT3_1	82	74.9	71.9	75.59
MP1_3	97	25.6	24.3	61.28
MP1_1	96	50.1	41.0	64.34
MP3_1	91	75.0	71.7	72.90

^a Obtained by measuring the elemental composition using an elemental analyser.

that the lower conversion rates/yields are related to the high improbability of limonene undergoing homopolymerisation.

A similar trend was observed for poly(carvone-*co*-TMPTA) and poly(carvone-*co*-PETA), where the yields decreased from 90%, to 74% and to 47% for the carvone-*co*-TMPTA system (CT1_3, CT1_1 and CT3_1, respectively) and from 95%, to 76% and to 54% for the carvone-*co*-PETA system (CP1_3, CP1_1 and CP3_1, respectively).

However, unlike limonene and carvone, β -myrcene has three double bonds with different reactivities which enables the homopolymerisation of myrcene and the synthesis of polymyrcene.^{29–31} Therefore, the yields of the myrcene-based polyHIPEs were significantly higher when compared to the limonene- and carvone-based polyHIPEs. The yields for poly(myrcene-*co*-TMPTA) ranged from 92% to 82%, while for poly(myrcene-*co*-PETA) they ranged from 97% to 91%.

The lower yields of the limonene- and carvone-based polyHIPEs were also correlated to the incorporation of the two terpenes into the polymer chain. As shown in Table 2, the incorporation of limonene was considerably lower from the limonene content in the monomer mixture prior the polymerisation. In the sample LT1_3 the measured limonene incorporation was 15.0 mol% which is approximately 10% lower from the theoretical value of 25.1 mol%. LT1_1 had a limonene content of 20.7 mol% (49.9 mol% theoretical) and LT3_1 a limonene content of 32.3 mol% (74.2 mol% theoretical). Based on these results the limonene incorporation drastically decreases by increasing its initial content in the HIPE mixture, which leads to both lower yields and a lower incorporation degree into the polymer network. However, these results were expected as limonene has low reactivity in radical homopolymerisation, while also reducing the rate of polymerisation

as shown by Sharma *et al.*^{27,32} These low polymerisation rates of limonene are related to the degradative chain transfer reaction due to the presence of the allylic C–H bond in limonene. Zhang *et al.* have shown this effect by copolymerising limonene with *n*-butyl methacrylate³³ and 2-ethylhexyl acrylate.³⁴ With the degradative chain transfer reaction further polymerisation is prevented resulting in the formation of low molecular weight polymers which are removed during the purification process. Through this process, both the low yields and low incorporation rates of limonene can be explained. In the case of the LP samples, LP1_3 had a limonene incorporation of 26.0 mol% which is similar to the theoretical value (25.1 mol%), while LP1_1 had a limonene incorporation of 27.6 mol% (50.2 mol% theoretical). However, LP3_1 had a considerably lower limonene content compared to other limonene-based samples, namely only 2.8 mol%. This indicates that the incorporation of limonene into the polymer chain was extremely low. This is most likely due to the higher reactivity and crosslinking density of PETA which prevents the polymerisation of limonene into the polymer chain at higher limonene ratios. Additionally, the same effect of the degradative chain transfer reaction is also present in these samples, however, it is evidently considerably more pronounced in the case of LP3_1 as the incorporation of limonene is only 2.8 mol% and less in pronounced the case of LP1_3 (25.1 mol% incorporation).

Like limonene, carvone also has low reactivity in radical homopolymerisation.³⁵ The incorporation of carvone into the copolymer (Table 2) in the case of the sample CT1_3 was almost 100%, as the theoretical value of carvone was 24.9 mol% and the measured values was 24.1 mol%. That value increased to 28.8 mol% in the case of CT1_1 (50.0 mol% theoretical) and decreased to 24.3% in the case of the sample CT3_1 (74.9 mol% theoretical). These values indicate that carvone has a maximum incorporation value in the poly(carvone-*co*-TMPTA) polyHIPE which is most likely related to the same degradative chain transfer reaction present in limonene, as carvone also contains an allylic C–H bond. A similar effect was also observed in the poly(carvone-*co*-PETA) polyHIPE which was also shown to have a maximum carvone content that can be achieved. The sample CP1_3 had a measured carvone content of 16.9 mol% (25.5 mol% theoretical), while the samples CP1_1 and CP3_1 had a carvone content of 25.0 and 24.1 mol%, respectively (50.4 and 74.8 mol% theoretical).

Unlike limonene and carvone, myrcene is more reactive (three double bonds) and also undergoes homopolymerisation to form polymyrcene.³⁰ Consequently, the measured myrcene content was almost identical to the theoretical values (Table 2). This higher reactivity and ability to homopolymerise is also reflected in the considerably higher yields which were mentioned previously.

Comparative FTIR spectra between the terpene-based polyHIPEs and the acrylate-only polyHIPEs are shown in the ESI (Fig. S1–S6†).

Thermogravimetric analysis (TGA) was conducted to evaluate the influence of the terpenes on the thermal decompo-



sition of the prepared polyHIPEs. The TGA graphs are shown in the ESI (Fig. S7–S12†). From the graphs it is evident that neither limonene nor carvone had any effect on the thermal decomposition of the polyHIPEs when compared to the acrylate-only polyHIPEs, however, in the case of the myrcene-based polyHIPEs a visible difference was observed in the case of MT3_1 and MP3_1. This indicates that a considerable amount of terpene is required to have an effect on the thermal decomposition of the samples. This possibly explains the identical graphs of the limonene- and carvone-based polyHIPEs, as the incorporation of limonene was at most 32.3 mol% and for carvone it was at most 28.8 mol%, which is considerably lower than the 71.9 mol% for MT3_1 and 71.7 mol% for MP3_1.

Morphology

The main property that determines the successful synthesis of polyHIPEs is their morphology. The morphology of polyHIPEs is defined by their interconnecting hierarchically porous structure consisting of primary pores (cavities) and interconnecting pores (windows). As a comparative material, pure PETA and TMPTA polyHIPEs were synthesised which are shown in Fig. 3.

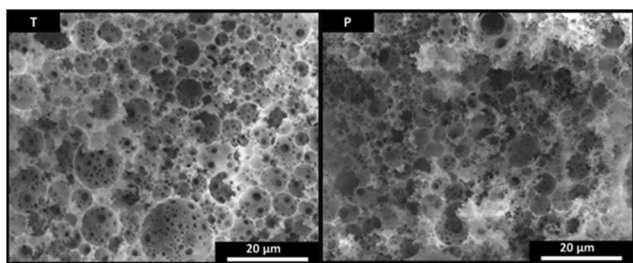


Fig. 3 Scanning electron microscopy (SEM) images of pure TMPTA and PETA.

Both materials had a typical polyHIPE morphology. Fig. 4–6 show that it was possible to synthesise terpene-based polyHIPEs from limonene, carvone and myrcene by using either TMPTA or PETA as the comonomers. However, it needs to be noted that the samples LP1_1 and LP3_1 did not produce a typical polyHIPE morphology, but instead formed a bicontinuous-like morphology, which will be discussed in the next section. Lastly, the average window diameter ($\langle d_{win} \rangle$) values are shown in Table 3 and will not be discussed as their values are approximately the same.

As already mentioned previously, it was possible to synthesise limonene-based polyHIPEs (Fig. 4). The average cavity diameter ($\langle D_{cav} \rangle$) of the poly(limonene-*co*-TMPTA) samples increased from $7.85 \pm 2.82 \mu\text{m}$ (LT1_3) to $9.14 \pm 3.06 \mu\text{m}$ (LT1_1) and lastly to $11.63 \pm 4.96 \mu\text{m}$ (LT3_1) with increasing limonene content. In comparison, the TMPTA-only polyHIPE had an $\langle D_{cav} \rangle$ of $8.57 \pm 3.90 \mu\text{m}$. The increase of the $\langle D_{cav} \rangle$ is most likely related to the polarity of the two monomers, which is lower in the case of limonene. The effect of the polarity was also shown by Barbetta *et al.* by using different solvents in the external phase to prepare styrene based polyHIPEs. The polyHIPEs prepared by using toluene as a solvent had a higher cavity diameter when compared to those prepared with either chlorobenzene or dichlorobenzene.²⁶ The poly(limonene-*co*-PETA) sample (LP1_3), had an $\langle D_{cav} \rangle$ of $5.51 \pm 1.55 \mu\text{m}$ which is comparable to the PETA-only polyHIPE ($\langle D_{cav} \rangle$ was $5.66 \pm 2.49 \mu\text{m}$). LP1_1 and LP3_1 did not produce a polyHIPE morphology, therefore, measuring the $\langle D_{cav} \rangle$ was not feasible.

Contrary to the $\langle D_{cav} \rangle$ the specific surface area (BET) decreased with increasing limonene content for both the TMPTA and PETA samples. The specific surface area of LT1_3 was $154.5 \text{ m}^2 \text{ g}^{-1}$, while the specific surface area for LT1_1 was $82.4 \text{ m}^2 \text{ g}^{-1}$ and $52.1 \text{ m}^2 \text{ g}^{-1}$ for LT3_1. In comparison, the TMPTA-only polyHIPE had a specific surface area of $91.7 \text{ m}^2 \text{ g}^{-1}$. These

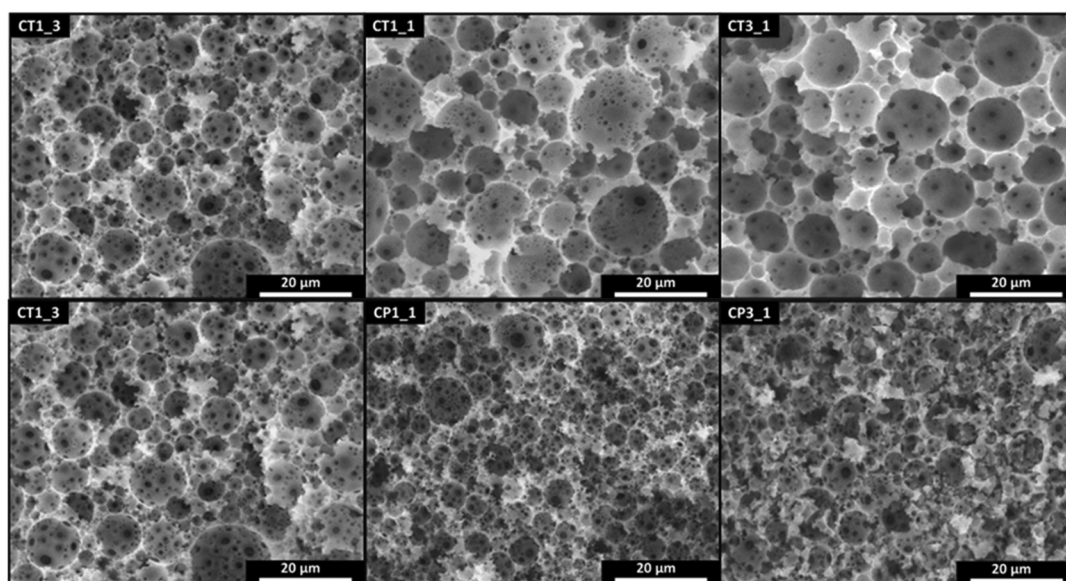


Fig. 4 Scanning electron microscopy (SEM) images of the limonene-based polyHIPEs.



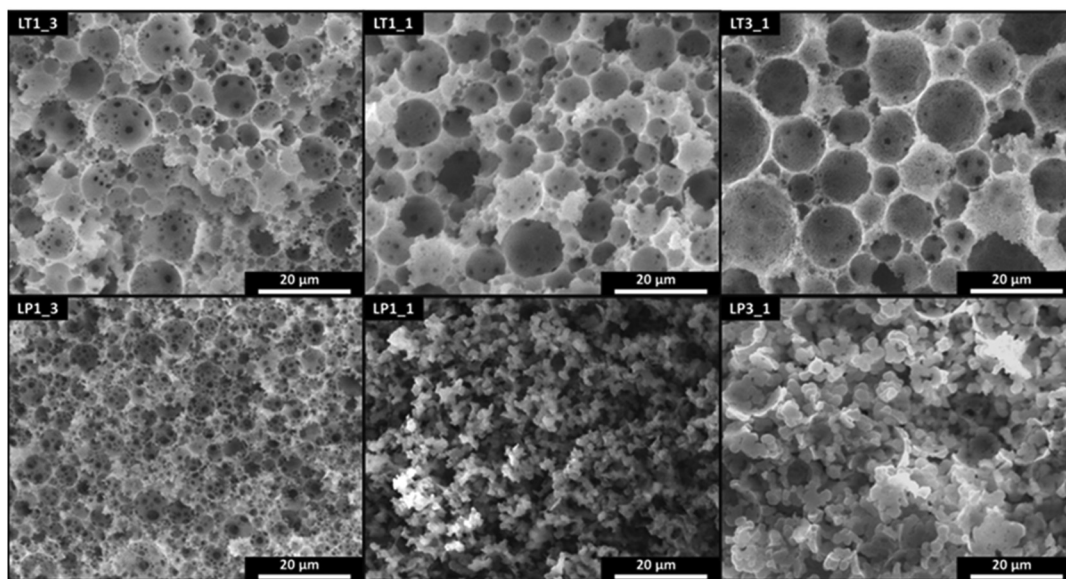


Fig. 5 Scanning electron microscopy (SEM) images of the carvone-based polyHIPEs.

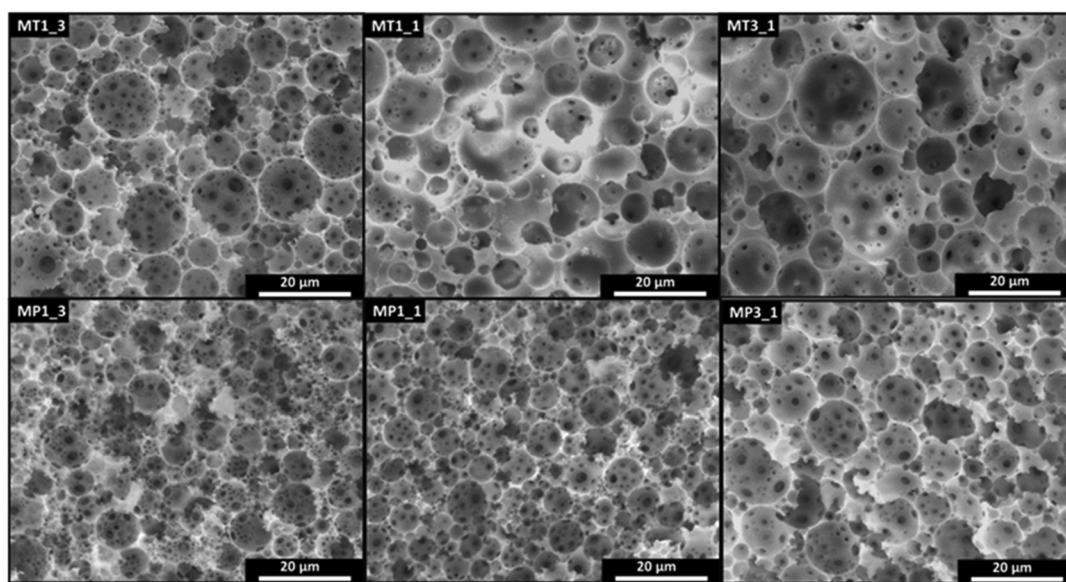


Fig. 6 Scanning electron microscopy (SEM) images of the myrcene-based polyHIPEs.

results indicate that a small addition of limonene increases the specific surface area of the terpene-containing polyHIPEs, while a greater limonene content decreases the specific surface area. The initial increase is probably a consequence of limonene acting as a porogenic solvent, while the decrease of the specific surface area with the increase of the limonene content, is most likely a consequence of the higher limonene content in the polymer and therefore, a lower crosslinking degree (limonene does not have as many reactive double bonds as TMPTA).

A similar trend was observed for the PETA samples, where the specific surface area of LP1_3 was $155.6 \text{ m}^2 \text{ g}^{-1}$, and only

$16.9 \text{ m}^2 \text{ g}^{-1}$ and $14.3 \text{ m}^2 \text{ g}^{-1}$ for LP1_1 and LP3_1, respectively. The PETA-only polyHIPE had a specific surface area of $301.5 \text{ m}^2 \text{ g}^{-1}$. The initial increase of the specific surface area in the case of the poly(limonene-co-TMPTA) samples does not occur in the poly(limonene-co-PETA) samples. This is probably due to a considerably higher limonene content in the sample LP1_3 (26.0 mol%) when compared to the sample LT1_3 (14.9 mol%). Consequently, limonene prevents the high crosslinking density usually present in poly(PETA), which results in a decrease of the specific surface area. The considerably lower specific surface areas of LP1_1 and LP3_1 are related to the bicontinuous structure obtained in those two samples. In a



Table 3 Porosity, specific surface area, average cavity and average window diameter of the prepared polyHIPEs

Sample	Porosity experimental ^a [%]	Porosity theoretical ^b [%]	BET [m ² g ⁻¹]	$\langle D_{\text{cav}} \rangle$ [μm]	$\langle d_{\text{win}} \rangle$ [μm]
LT1_3	87.0%	87.6%	154.5	7.85 ± 2.82	0.75 ± 0.32
LT1_1	91.1%	87.2%	82.4	9.14 ± 3.06	0.82 ± 0.30
LT3_1	93.8%	86.8%	52.1	11.63 ± 4.96	0.71 ± 0.33
LP1_3	90.5%	87.9%	155.6	5.51 ± 1.55	0.89 ± 0.39
LP1_1	N/A	87.6%	16.9	N/A	N/A
LP3_1	N/A	87.2%	14.3	N/A	N/A
CT1_3	86.9%	87.7%	63.4	8.77 ± 4.64	0.87 ± 0.51
CT1_1	84.9%	86.8%	118.1	9.67 ± 4.64	0.86 ± 0.33
CT3_1	87.8%	87.3%	121.2	9.59 ± 3.96	0.87 ± 0.30
CP1_3	86.7%	88.3%	256.8	7.80 ± 2.23	1.01 ± 0.55
CP1_1	91.1%	88.0%	279.3	7.26 ± 2.52	0.84 ± 0.40
CP3_1	94.8%	87.6%	296.8	8.94 ± 3.63	0.70 ± 0.48
MT1_3	86.7%	87.5%	11.4	8.25 ± 3.70	0.84 ± 0.58
MT1_1	82.0%	87.2%	3.3	9.22 ± 3.46	0.75 ± 0.34
MT3_1	84.4%	86.8%	2.7	11.24 ± 4.75	0.95 ± 0.51
MP1_3	87.7%	87.8%	192.0	8.14 ± 2.38	0.92 ± 0.50
MP1_1	87.1%	87.4%	18.1	7.93 ± 1.92	0.97 ± 0.41
MP3_1	86.5%	87.0%	5.7	10.47 ± 3.34	0.96 ± 0.55
T	89.7%	87.7%	91.72	8.57 ± 3.90	0.89 ± 0.44
P	88.2%	88.2%	301.54	5.66 ± 2.49	0.81 ± 0.52

^aThe experimental porosity was determined by measuring the overall density and skeletal density. ^bThe theoretical porosity was calculated by taking both the internal phase volume and the solvent volume into account.

study conducted by Paljevac *et al.*³⁶ it was shown that polymers with a bicontinuous-like morphology had lower specific surface areas than their analogues prepared with high internal phase emulsion templating, which also explains the significantly lower specific surface area in the case of the limonene-based polymers LP1_1 and LP3_1.

Lastly, as the prepared samples were porous, it was necessary to measure their porosities which are shown in Table 3. The porosities of the prepared limonene-based polyHIPEs were expected to be approximately 87% (Table 3). LT1_3 had a porosity of 87.05% which is similar to the theoretical value. However, the samples LT1_1 and LT3_1 had slightly higher experimental porosities (91.1% and 93.8%). This is due to the lower limonene content in the samples LT1_1 and LT3_1 which resulted in the limonene having the role of the solvent and contributing to the higher porosities of the prepared samples. The porosity for the samples LP1_1 and LP3_1 was not determined as they were too brittle to be measured with the established method.

Another newly synthesised polyHIPE was the carvone-based one. The $\langle D_{\text{cav}} \rangle$ of the poly(carvone-*co*-TMPTA) polyHIPEs was approximately the same across all of the synthesised samples ranging from 8.77 μm to 9.67 μm (Table 3). This is most likely due to the identical composition of the polyHIPEs as determined by the carvone incorporation. A similar trend is present in the poly(carvone-*co*-PETA) polyHIPEs where the $\langle D_{\text{cav}} \rangle$ ranges from 7.26 to 8.94 μm. In comparison, the $\langle D_{\text{cav}} \rangle$ of poly(TMPTA) and poly(PETA) were 8.57 μm and 5.66 μm, respectively.

Unlike in the case of the limonene-based polyHIPEs, the carvone-based polyHIPEs were observed to have an increased

specific surface area with increasing carvone content in the initial HIPE (from 63.4 to 121.2 m² g⁻¹ (CT samples); from 256.8 to 296.8 m² g⁻¹ (CP samples); Table 3). This is most likely due to the fact, that the carvone content in the synthesised samples was approximately the same, which resulted in the remaining carvone having the role of a porogenic solvent, therefore, increasing the overall specific surface area of the prepared polyHIPEs. The effect of a porogenic solvent (chlorobenzene) was also demonstrated by Barbetta *et al.*³⁷ with the increase of the volume of chlorobenzene which increased the surface area. It needs to be noted that the poly(carvone-*co*-TMPTA) polyHIPEs had a higher specific surface area in the case of the samples CT1_1 and CT3_1 when compared to the TMPTA-only polyHIPE (91.7 m² g⁻¹) due to the porogenic solvent, however, while a similar trend was present in the CP samples, all of the specific surface area values were slightly below the PETA-only polyHIPE (301.5 m² g⁻¹). These results indicate that the addition of carvone lowers the specific surface area of PETA-based polyHIPEs, despite its role as a porogenic solvent. This is most likely due to the overall lower crosslinking degree due to the presence of carvone, which was also demonstrated by Nodehi *et al.* in a styrene-divinylbenzene system. By increasing the divinylbenzene ratio, the specific surface area of the prepared polymers was increased.³⁸

Lastly, the porosities of the prepared carvone-based polyHIPEs for the CT samples were similar to the theoretical values (Table 3), while the CP samples had slightly higher experimental values.

The $\langle D_{\text{cav}} \rangle$ of the myrcene-based polyHIPEs increased slightly in both the MT and MP samples with increasing myrcene content. The $\langle D_{\text{cav}} \rangle$ of the MT samples ranged from



8.25 to 11.24 μm , while the $\langle D_{\text{cav}} \rangle$ of the MP samples ranged from 7.93 to 10.47 μm (Table 3).

The specific surface area of the MT samples was significantly lower from the specific surface area from all the other terpene-based and acrylate-only samples. It decreased from 11.4 $\text{m}^2 \text{g}^{-1}$ to 2.7 $\text{m}^2 \text{g}^{-1}$ with increasing myrcene content (from 25 to 75 mol%), which was expected, due to the considerably lower crosslinking degree. Additionally, unlike limonene and carvone, the incorporation of myrcene into the polyHIPE was close to the theoretical values, meaning that myrcene did not act as a porogenic solvent and was solely acting as a polymerisable entity. The same trend is present in the MP samples, albeit with significantly higher specific surface areas due to the higher crosslinking density of PETA. In the case of MP1_3 the specific surface area was 192.0 $\text{m}^2 \text{g}^{-1}$ and in the case of MP1_1 and MP3_1 it decreased to 18.1 and 5.7 $\text{m}^2 \text{g}^{-1}$, respectively.

Lastly, the measured porosities of the samples were similar to the theoretical ones, which was also expected as almost the entire myrcene polymerised into the polymer chain.

By combining terpenes with either TMPTA or PETA it was possible to synthesise polyHIPEs with partial bio-based content. Additionally, the synthesised polyHIPEs had high specific surface areas ranging up to approximately 300 $\text{m}^2 \text{g}^{-1}$. This usually is not the case for polyHIPEs, as their specific surface areas are generally in the tens of $\text{m}^2 \text{g}^{-1}$. To achieve a specific surface area in the hundreds, hypercrosslinking is often required.³⁹

Conclusion

This study shows that it is possible to synthesise hierarchically porous polyHIPEs from limonene, carvone and myrcene by using multifunctional acrylates as the co-monomers. It was shown that the increase of the terpene content decreases the overall yield of the polymerisation. However, it was still possible to get relatively high incorporation degrees of both limonene and carvone, while the incorporation of myrcene into the polymer chain was close to the theoretical values. The synthesised polyHIPEs had high specific surface areas up to 300 $\text{m}^2 \text{g}^{-1}$, which is usually not common for polyHIPEs, while the porosities of the polymers ranged from 82.0% and up to 94.8%. Lastly, the average cavity diameter ranged from 5.51 μm to 11.24 μm . This work shows that various terpenes can be used to synthesise partially bio-based highly porous polymers with high specific surface areas.

Author contributions

Stanko Kramer: conceptualisation; data curation; formal analysis; investigation; methodology; visualisation; writing – original draft. Nika Skušek: data curation; investigation; methodology; visualisation. Peter Krajnc: conceptualisation, funding acquisition; supervision; writing – review & editing.

Conflicts of interest

There are no conflicts to declare.

Acknowledgements

This work was supported by the Slovenian Research Agency (ARRS) through the research programme P2-0006 and scholarship to SK.

References

- 1 European Bioplastics, nova-Institute (2022), Bioplastics market data, <https://www.european-bioplastics.org/market/>, (accessed 5th December 2022).
- 2 PlasticsEurope (PEMRG). “Annual production of plastics worldwide from 1950 to 2021 (in million metric tons)” Chart. December 2, 2022. Statista. (Accessed 11th December 2022).
- 3 F. Perera and K. Nadeau, *N. Engl. J. Med.*, 2022, **386**, 2303–2314.
- 4 R. M. Cywar, N. A. Rorrer, C. B. Hoyt, G. T. Beckham and E. Y. X. Chen, *Nat. Rev. Mater.*, 2022, **7**, 83–103.
- 5 G. Crini, *Prog. Polym. Sci.*, 2005, **30**, 38–70.
- 6 G. Férey, *Chem. Soc. Rev.*, 2008, **37**, 191–214.
- 7 X. Lu, W. Zhang, C. Wang, T. C. Wen and Y. Wei, *Prog. Polym. Sci.*, 2011, **36**, 671–712.
- 8 D. Wang, Y. Jin, X. Zhu and D. Yan, *Prog. Polym. Sci.*, 2017, **64**, 114–153.
- 9 H. Tian, Z. Tang, X. Zhuang, X. Chen and X. Jing, *Prog. Polym. Sci.*, 2012, **37**, 237–280.
- 10 D. Wu, F. Xu, B. Sun, R. Fu, H. He and K. Matyjaszewski, *Chem. Rev.*, 2012, **112**, 3959–4015.
- 11 N. R. Cameron, *Polymer*, 2005, **46**, 1439–1449.
- 12 T. Zhang, R. A. Sanguramath, S. Israel and M. S. Silverstein, *Macromolecules*, 2019, **52**, 5445–5479.
- 13 M. De Colli, M. Massimi, A. Barbetta, B. L. Di Rosario, S. Nardecchia, L. Conti Devirgiliis and M. Dentini, *Biomed. Mater.*, 2012, **7**, 055005.
- 14 A. Barbetta, M. Dentini, M. S. De Vecchis, P. Filippini, G. Formisano and S. Caiazza, *Adv. Funct. Mater.*, 2005, **15**, 118–124.
- 15 S. Zhou, A. Bismarck and J. H. G. Steinke, *J. Mater. Chem. B*, 2013, **1**, 4736–4745.
- 16 L. Avraham, R. A. Sanguramath, O. Cohen, L. Perry, S. Levenberg and M. S. Silverstein, *Eur. Polym. J.*, 2022, **169**, 111140.
- 17 S. Kramer, N. R. Cameron and P. Krajnc, *Polymers*, 2021, **13**, 1–24.
- 18 T. Yang, Y. Hu, C. Wang and B. P. Binks, *ACS Appl. Mater. Interfaces*, 2017, **9**, 22950–22958.
- 19 A. Foulet, M. Birot, G. Sonnemann and H. Deleuze, *React. Funct. Polym.*, 2015, **90**, 15–20.



- 20 Y. Zhu, C. Romain and C. K. Williams, *Nature*, 2016, **540**, 354–362.
- 21 P. A. Wilbon, F. Chu and C. Tang, *Macromol. Rapid Commun.*, 2013, **34**, 8–37.
- 22 E. H. Mert and B. Kekevi, *Colloid Polym. Sci.*, 2020, **298**, 1423–1432.
- 23 B. Kekevi and E. H. Mert, *Eur. Polym. J.*, 2021, **152**, 110474.
- 24 B. Kekevi and E. H. Mert, *J. Appl. Polym. Sci.*, 2021, **138**, 1–13.
- 25 B. Kekevi and E. H. Mert, *React. Funct. Polym.*, 2021, **164**, 104912.
- 26 A. Barbetta and N. R. Cameron, *Macromolecules*, 2004, **37**, 3188–3201.
- 27 S. Sharma and A. K. Srivastava, *Indian J. Chem. Technol.*, 2005, **12**, 62–67.
- 28 S. Ren, E. Trevino and M. A. Dubé, *Macromol. React. Eng.*, 2015, **9**, 339–349.
- 29 A. C. Weems, K. R. Delle Chiaie, R. Yee and A. P. Dove, *Biomacromolecules*, 2020, **21**, 163–170.
- 30 P. Sarkar and A. K. Bhowmick, *RSC Adv.*, 2014, **4**, 61343–61354.
- 31 J. L. Cawse, J. L. Stanford and R. H. Still, *J. Appl. Polym. Sci.*, 1986, **31**, 1963–1975.
- 32 S. Sharma and A. K. Srivastava, *Polym.-Plast. Technol. Eng.*, 2003, **42**, 485–502.
- 33 Y. Zhang and M. A. Dubé, *Macromol. React. Eng.*, 2014, **8**, 805–812.
- 34 Y. Zhang and M. A. Dubé, *Polym.-Plast. Technol. Eng.*, 2015, **54**, 499–505.
- 35 T. Nishida, K. Satoh, S. Nagano, T. Seki, M. Tamura, Y. Li, K. Tomishige and M. Kamigaito, *ACS Macro Lett.*, 2020, **9**, 1178–1183.
- 36 M. Paljevac, J. Kotek, K. Jeřábek and P. Krajnc, *Macromol. Mater. Eng.*, 2018, **303**, 1–8.
- 37 A. Barbetta and N. R. Cameron, *Macromolecules*, 2004, **37**, 3202–3213.
- 38 A. Nodehi, M. Hajiebrahimi, M. Parvazinia, M. Shahrokhi and H. Abedini, *J. Appl. Polym. Sci.*, 2011, **120**, 1942–1949.
- 39 A. Koler, I. Pulko and P. Krajnc, *Acta Chim. Slov.*, 2020, **67**, 349–360.

